Electronic Supplementary Material (ESI) for ChemComm.

– SUPPORTING INFORMATION –

Polyol-mediated C-Dot Formation showing Efficient Tb^{3+}/Eu^{3+} Emission

Hailong Dong[a], Ana Kuzmanoski[a], Dorothee M. Gößl[a], Radian Popescu[b], Dagmar Gerthsen[b], and Claus Feldmann*[a]

[a] Institut für Anorganische Chemie,
Karlsruhe Institute of Technology (KIT)
Engesserstrasse 15, 76131 Karlsruhe, Germany

[b] Laboratorium für Elektronenmikroskopie,
Karlsruhe Institute of Technology (KIT)
Engesserstrasse 7, 76131 Karlsruhe, Germany

1. Analytical tools

a) Transmission electron microscopy (TEM): Transmission electron microscopy (TEM) and high-resolution transmission electron microscopy (HRTEM) were performed with an aberration-corrected FEI Titan^3 80-300 microscope operated at 300 kV. TEM samples were prepared by evaporating suspensions in ethanol on amorphous carbon (Lacey-)film suspended on copper grids. The deposition of the samples on the carbon (Lacey-)film copper grids was performed under Argon atmosphere in a glove-box. Average particle diameters were calculated by statistical evaluation of at least 150 particles (Scandium 5.0 software package, Soft Imaging Systems).

b) Fluorescence spectroscopy (FL) and determination of quantum yield: Excitation and emission spectra were recorded using a photoluminescence spectrometer Horiba Jobin Yvon Spex Fluorolog 3, equipped with a 450 W Xenon lamp, double monochromators, Ulbricht sphere and photomultiplier as detector (90 ° angle between excitation source and detector). Determination of the absolute quantum yield was performed as suggested by *Friend*.[1] First, the diffuse reflection of the sample was determined under excitation. Second, the emission was measured for the respective excitation wavelength. Integration over the reflected and emitted photons in wavelength range of 400–700 nm by use of an Ulbricht sphere allows calculating the absolute quantum yield. Standard corrections were used for the spectral power of the excitation source, the reflection behaviour of the Ulbricht sphere and the sensitivity of the detector. All quantum yields were obtained for dispersions of the C-dots in D_2O that were adjusted to an absorbance of 0.1. The sample holder for determining the absolute quantum yield of suspensions in an Ulbricht sphere was constructed according to *Friend* and is shown in Figure S1.[1]

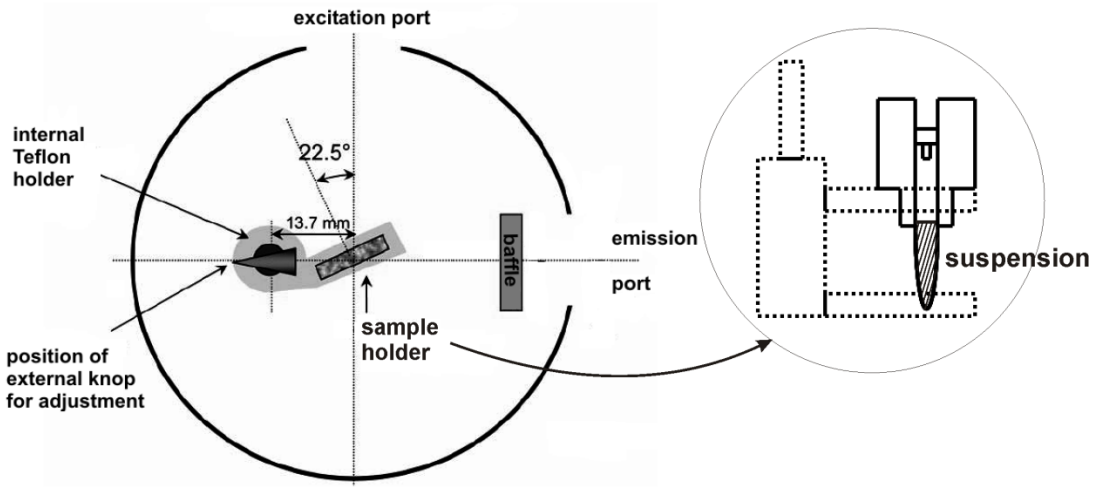

Figure S1. Sample holder for determining the absolute quantum yield of suspensions in an Ulbricht sphere according to *Friend*.[1]

c) Blue light emitting diode (blue-light LED): A *blue-LED light source* (LED lenser) was purchased by Zweibrüder Optoelectronics. The blue-LED exhibited a total length of 66 mm, a diameter of 14 mm and a total weight of 19 g. It operated with 12 lm at a wavelength range of 440–500 nm and with λ_{max} = 465 nm (*Fig. S2*).

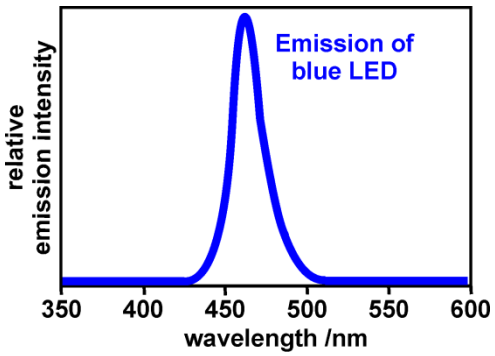

Figure S2. Emission spectrum of the applied blue-light LED.

d) X-ray powder diffraction (XRD): X-ray powder diffraction (XRD) was performed with a Stoe STADI-P diffractometer operating with Ge-monochromatized Cu-Kα-radiation (λ = 1.54178 Å) and Debye-Scherrer geometry.

e) Infrared spectroscopy (FT-IR): Fourier-transform infrared spectra were recorded on a Bruker Vertex 70 FT-IR spectrometer using KBr pellets.

2. C-dot characterization

a) General considerations

The characterization of C-dots, especially, addresses conditions of synthesis, colloidal properties, chemical composition, and photoluminescence. This includes particle size, size distribution, crystallinity, and surface conditioning of the C-dots. The fluorescence properties were investigated in view of a correlation with the type of polyol, the presence of metal salts, the temperature of heating, and the duration of heating. In fact, this variety of aspects spans a parameter box that can be hardly addressed completely on the timescale of this work. Thus, we have focused on those parameters that result in C-dots of the highest fluorescence intensity and quantum yield. A systematic variation of all optional parameters–in fact, there are even more than considered in this work–needs much more time.

b) Chemical composition of the as-prepared C-dots

Subsequent to acetone-driven destabilization, separation and washing of the as-prepared C-dots, electron microscopy (TEM, HRTEM, *cf. main paper: Fig. 2*), X-ray powder diffraction (XRD, Fig. S3a), and Fourier-transformed infrared spectroscopy (FT-IR, Fig. S3b) were performed. The crystallinity is demonstrated by HRTEM (*cf. main paper: Fig. 2b*) and Fourier-transformed HRTEM images of single C-dots (*cf. main paper: Fig. 2c*). XRD confirms the crystallinity of the as-prepared C-dots as well. The observed Bragg peaks are well in accordance with bulk-graphite (Fig. 32a).[2] Due to the small particle and crystallite size of 3–5 nm as well as due to the resulting stress and strain effects, all Bragg peaks exhibit low intensities, broad peak widths and a certain shift to lower 2-Theta angles as compared to bulk-graphite. As the bonding between the carbon layers is limited to weak van-der-Waals interactions, the shift of Bragg peaks is most obvious for *(hkl)* indices of the *(00l)* type. Thus, the observed significant shift of the *(002)* Bragg peak at about 20 ° of 2-Theta is to be expected.

Since the C-dots were prepared in pure polyols as solvents, the surface of the as-prepared C-dots is inherently coated by the polyol. Thus, FT-IR spectra of C-dots from refluxed PEG400 (230 °C, 1 h) show the characteristic vibrations of PEG400 with ν(O–H) (3600-3100 cm^{-1}), ν(C–H) (3000-2800 cm^{-1}), ν(C–O) (1200-1000 cm^{-1}), and the fingerprint with weak δ(C–H)/δ(C–C) vibrations in the 1400 to 750 cm^{-1} range. The observed vibrations are well in accordance with pure, non-heated PEG400 as a reference. In addition, the C-dots exhibit a strong absorption at 1500-1400 cm^{-1} (Fig. S3b). This vibration can be ascribed to ν(C=O) and indicates the beginning dehydration and carbonization of the polyol. Additional vibrations at 1750–1600 cm^{-1} are indicative of aromatic C=C bonds and confirm the formation of graphite-type C-dots. These findings are well in agreement with FT-IR spectra of post-synthesis polyol-stabilized C-dots as reported in the literature.[3]

XRD patterns and FT-IR spectra as shown in Figure S3 are representative for all C-dots obtained here via polyol-mediated synthesis.

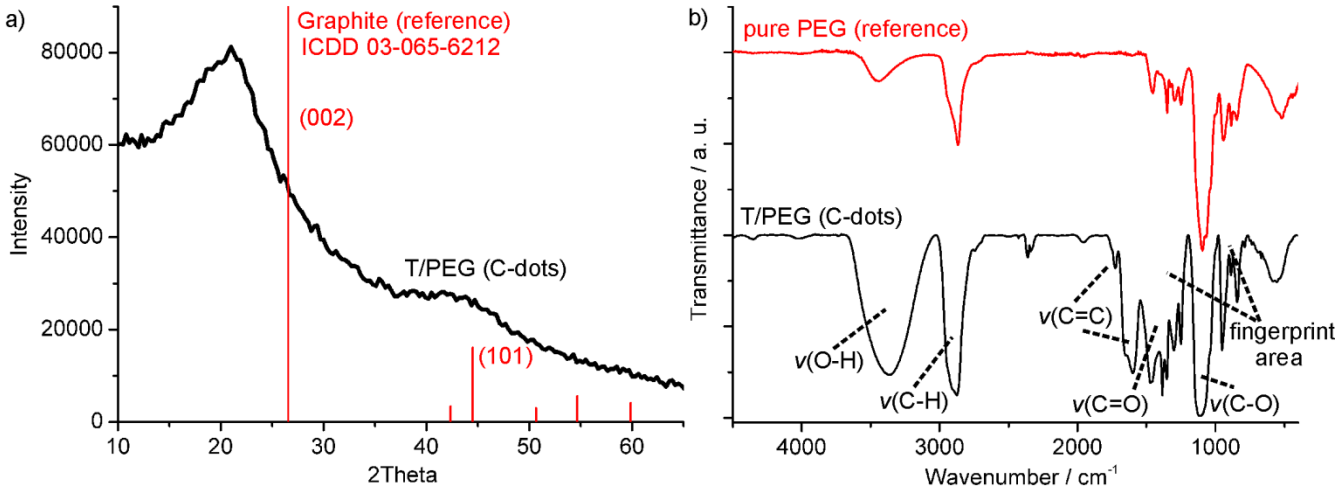

Figure S3. X-ray powder diffraction pattern (XRD) (a) and Fourier-transformed infrared spectrum (b) of as-prepared C-dots (PEG400, 230 °C, 1 h) (ICDD 03-065-6212/bulk-graphite, and FT-IR spectrum of pure PEG400 as a references).

c) Colloidal properties and separation of the as-prepared C-dots

The polyol-mediated formation of C-dots resulted in highly viscous, brownish suspensions (Fig. S4). These as-prepared C-dots can be directly dispersed in water by dropping the C-dot suspension to water under intense stirring. The ratio of the C-dot suspension and water is optimal at about 1 : 30. The resulting light brown suspensions show intense blue emission if the pure polyol was refluxed (*cf. main paper: Fig. 1b*). In the presence of $MgCl_2{\times}6H_2O$, $TbCl_3{\times}6H_2O$ or $EuCl_3{\times}6H_2O$ intense yellow (*cf. main paper: Fig. 1c*), green (*cf. main paper: Fig. 1d*), and red (*cf. main paper: Fig. 1e*) emission is observed. All these aqueous suspensions exhibit excellent colloidal stability with mean particle diameters of 3–5 nm at narrow size distribution (Fig. S4, *cf. main paper: Fig. 2*).

Alternatively, the as-prepared C-dot suspensions can be destabilized by addition of acetone with a ratio of 1 : 10. After about 12 h, the C-dots are collected at the bottom of the flask by natural sedimentation. After sequential decantation of the supernatant, redispersion in acetone and sedimentation, a light greyish powder was obtained, and finally dried in a drying oven for 30 min at 80 °C (Fig. S4). This C-dot powder is obtained in quantities of about 20 mg C-dots per 10 ml of the polyol. Powder samples are used for materials analysis, including XRD and FT-IR (Fig. S3).

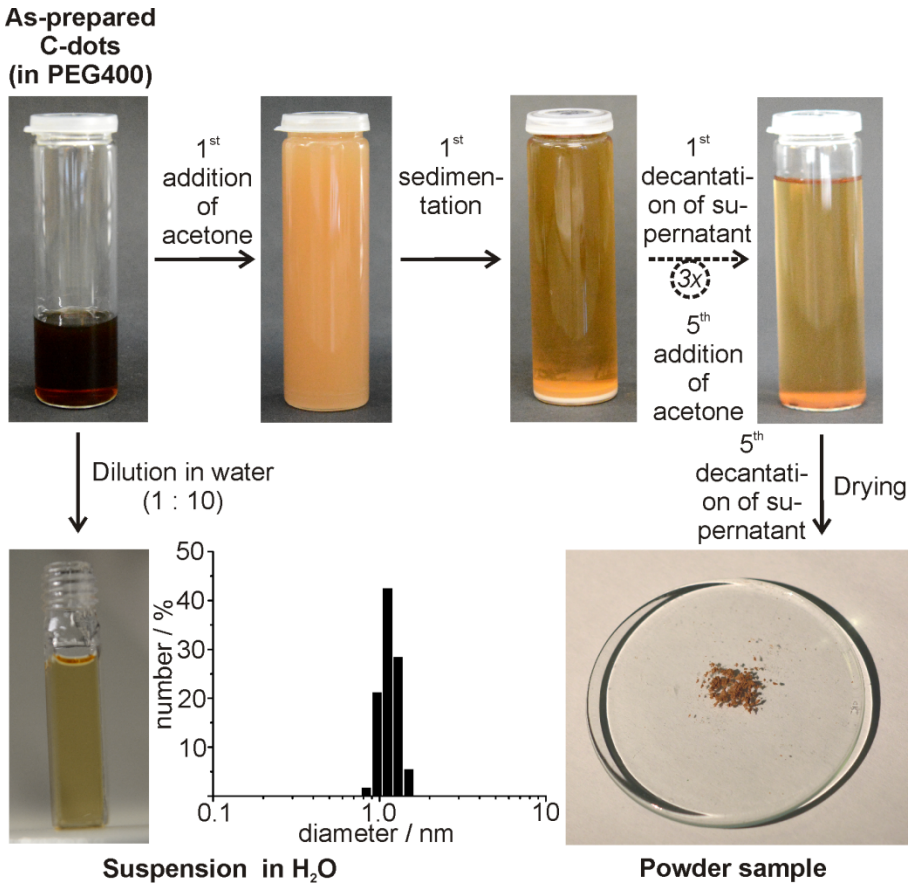

Figure S4. Photos showing suspensions of the as-prepared C-dots (PEG400, 230 °C, 1 h) and the direct dispersion in water (with size and size distribution according to DLS analysis) as well as the purification and sedimentation procedure for obtaining powder samples.

d) Effect of the type of polyol and the presence of metal salts on the as-prepared C-dots

The as-prepared C-dots show broad absorption in a range of 300 to 400 nm (Fig. S5). Excitation spectra of the different polyols after heating for 1 h to 230 °C (Fig. S5a) and of the different polyols after heating for 1 h to 230 °C in the presence of 0.5 mmol $MgCl_2{\times}6H_2O$ or $ZnCl_2$ (Fig. S5b) were normalized on maximum intensity in order to allow for direct comparison of the emission intensity (*cf. main paper: Fig. 3*). Whereas the width of the excitation is more-or-less similar for all samples, the position of maximum absorption shows a clear correlation to the type of the polyol and the type of added cation. Accordingly, the absorption is red-shifted at higher molecular weight of the polyol in the sequence GLY < DEG < PEG400 with the excitation maxima at 337, 352, and 369 nm (Fig. S5a). This red-shift is even stronger when refluxing the polyol in the presence of $MgCl_2{\times}6H_2O/ZnCl_2$ with Mg^{2+}/GLY having its maximum absorption at 329 nm, and Zn^{2+}/PEG having its maximum absorption at 387 nm (Fig. S5b). A similar correlation to molecular weight is also observed for the emission

intensity (*cf. main paper: Fig. 3*). In view of the position of maximum emission, the type of the polyol as well as the type of added metal salt have a minor influence only.

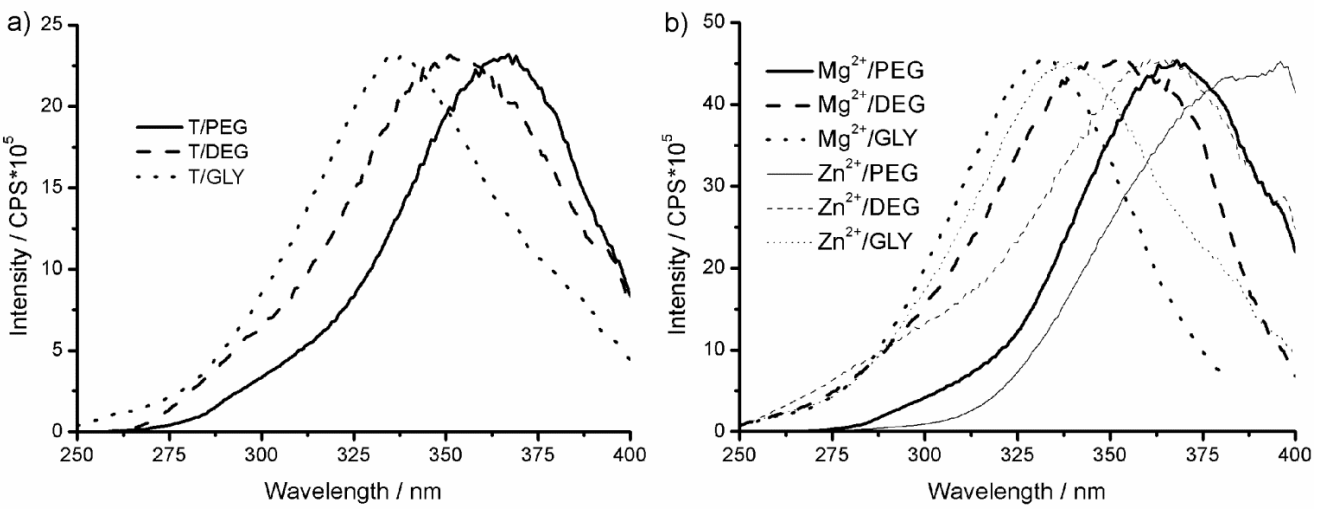

Figure S5. Normalized C-dot excitation after most simple refluxing of: a) pure GLY, DEG and PEG400; b) GLY, DEG, PEG400 with dissolved $MgCl_2{\times}6H_2O/ZnCl_2$ (230 °C, 1 h, 0.5 mmol $MgCl_2{\times}6H_2O/ZnCl_2$).

As the type of the polyol and the presence of $MgCl_2{\times}6H_2O/ZnCl_2$ clearly influence the fluorescence of the as-prepared C-dots (Fig. S4, *cf. main paper: Fig. 3*), different concentrations of the metal salts have been used, too. To this concern, we evaluated $MgCl_2{\times}6H_2O$ with concentrations of 0.05, 0.50, and 2.0 mmol (Fig. S6). Upon excitation at different wavelengths, emission intensity, position of maximum intensity, and width of emission band remain very comparable. Accordingly, just the presence of the metal salt is most relevant; increasing the metal salt concentration is only of minor influence.

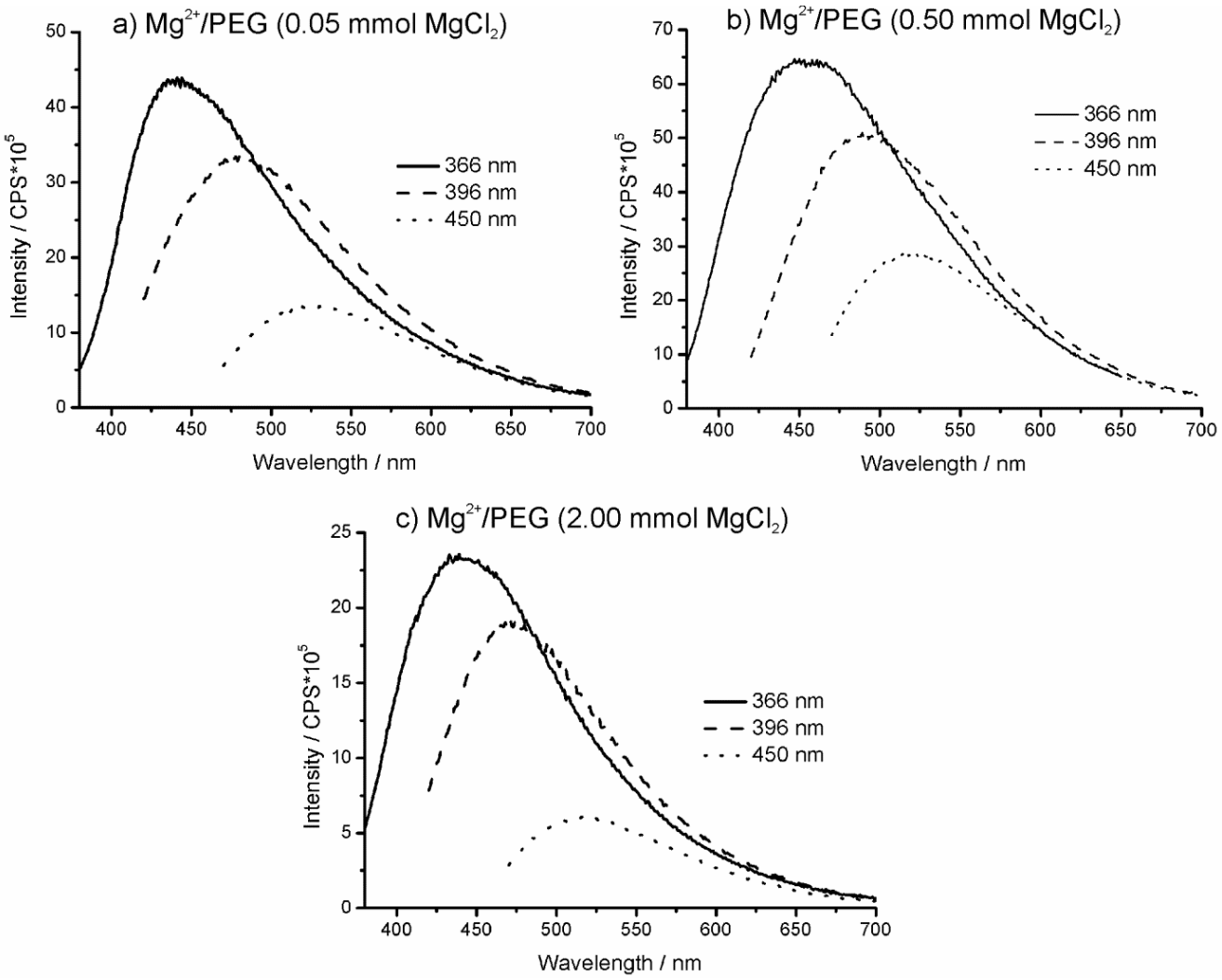

Figure S6. Effect of different concentrations of $MgCl_2 \times 6H_2O$ (0.05, 0.50, 2.00 mmol) on the emission intensity of C-dots as-prepared in PEG400 (230 °C, 1 h).

e) Effect of the temperature of heating on the as-prepared C-dots

Besides the influence of the polyol and the concentration of the metal salt, the effect of the temperature of heating and refluxing was studied. To this concern, PEG400 was selected as it shows the highest emission intensities. For comparison, three different temperatures have been studied: 150 °C (Fig. S7a), 190 °C (Fig. S7b), and 230 °C (Fig. S7c). Up to a temperature of 150 °C, only weak emission in the blue spectral range (400–550 nm) is observed. Thus, dehydration and carbonization of the polyol have just started as indicated by a light yellow colour of the suspensions (Fig. S7a). Number and quality of the C-dots remain at low level. Increasing the temperature to 190 °C results in a light brown colour of the suspensions and a four-times higher emission intensity (Fig. S7b). The colour shift now ranges from blue to orange (400–650 nm). By heating at 230 °C, the colour of the suspensions turned to dark

brown indicating the proceeding dehydration and carbonization of the polyols (Fig. S7c). The fluorescence intensity is further increased, and–depending on the wavelength of the excitation–the emission now covers the complete optical spectrum (400–700 nm). At even higher temperatures (> 230 °C) decomposition of the polyols became very fast and less controlled. The resulting deep black suspensions exhibited significantly reduced fluorescence intensities as compared to suspensions refluxed at 230 °C. The quality of the C-dots in terms of particle size, size distribution, and agglomeration was decreased as well.

f) Effect of the duration of heating on the as-prepared C-dots

In addition to the influence of the polyol, the concentration of the added metal salt, and the temperature of refluxing, we have studied the duration of heating. Again, PEG400 showing the highest emission intensities was selected. Since typical experiments were performed by heating for 1 h at 230 °C, the temperature was maintained but the duration of heating was extended from 1 h to 2 and 6 hours (Fig. S8). Comparing the resulting emission spectra, again, a certain red-shift of the emission is visible at increased duration of heating. In comparison to the temperature of heating (Fig. S7), however, the duration of heating only has a minor influence on the fluorescence intensity and the colour shift (Fig. S8).

In sum, the polyol-mediated synthesis of C-dots–according to our studies–is best performed by heating PEG400 for 1 h at 230 °C in the presence of a low amount of $MgCl_2 \times 6H_2O$ (0.05 mmol).

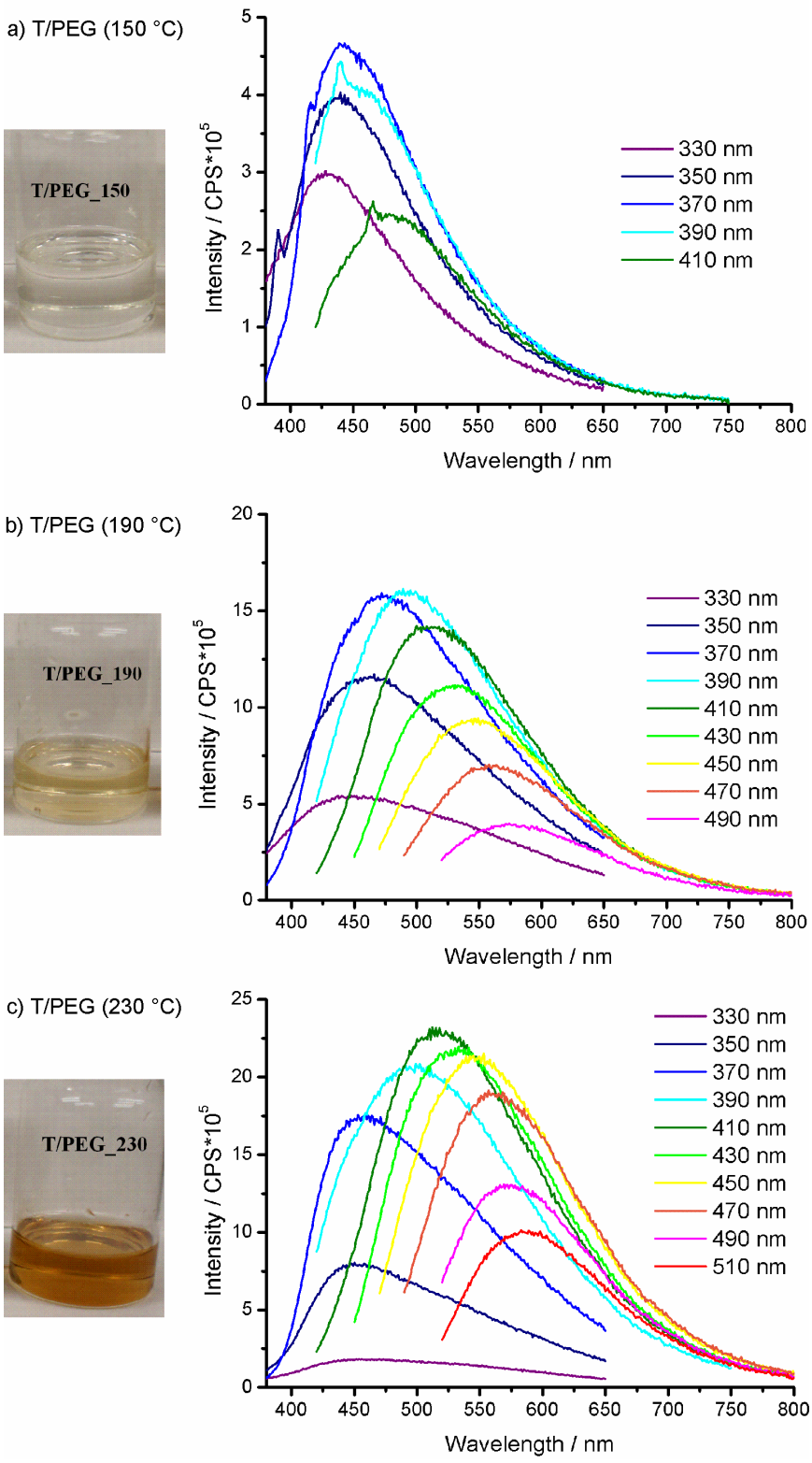

Figure S7. Effect of temperature (150, 190, 230 °C) on emission intensity and colour shift of C-dots as-prepared in PEG400: a) Photo and emission spectra of PEG400 refluxed at 150 °C; b) Photo and emission spectra of PEG400 refluxed at 190 °C; c) Photo and emission spectra of PEG400 refluxed at 230 °C (all samples heated for 1 h at the respective temperature).

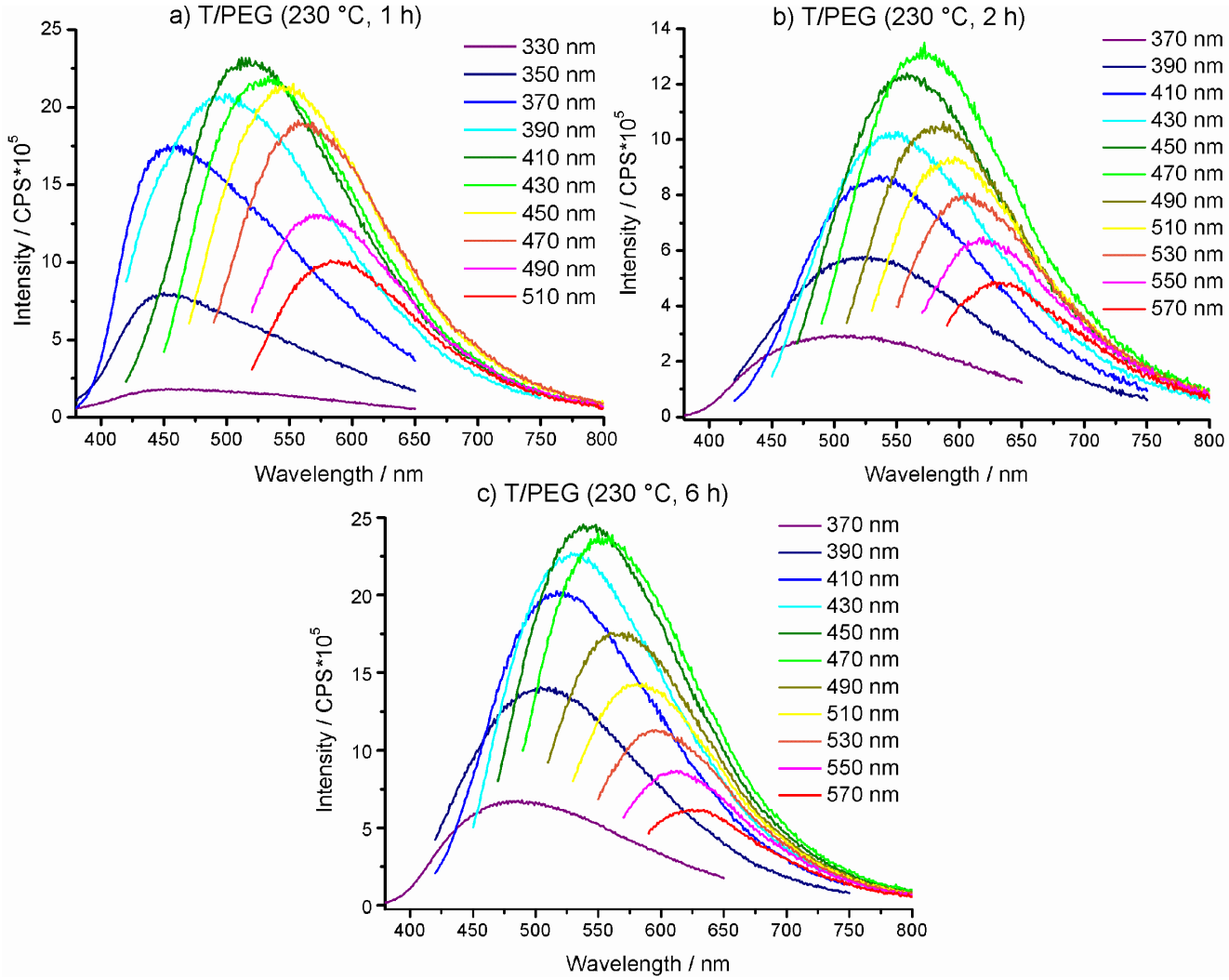

Figure S8. Effect of duration of heating (1, 2, 6 h) on emission intensity and color shift of C-dots as-prepared in PEG400: a) Emission spectra of PEG400 refluxed for 1 h; b) Emission spectra of PEG400 refluxed for 2 h; c) Emission spectra of PEG400 refluxed for 6 h (all samples heated to 230 °C for the respective duration).

g) Effect of the addition of $TbCl_3 \times 6H_2O$ and $EuCl_3 \times 6H_2O$ on the as-prepared C-dots

As the addition of $MgCl_2 \times 6H_2O$ and $ZnCl_2$ resulted in enhanced fluorescence intensities of the as-prepared C-dots, we intended achieving a similar effect upon addition of $TbCl_3 \times 6H_2O$ or $EuCl_3 \times 6H_2O$. Since Tb^{3+} and Eu^{3+} are well-known for their characteristic line-type $f \rightarrow f$ transitions, we also aimed at a Förster resonance energy transfer (FRET) from the C-dot to surface-allocated Tb^{3+}/Eu^{3+}. Surprisingly, excitation of the Tb^{3+}/Eu^{3+}-modified C-dots indeed shows intense characteristic, line-type $f \rightarrow f$ transitions of the rare-earth metals (Fig. S9; *cf. main paper: Fig. 5*). This is validated here for refluxing

PEG400 (230 °C, 1 h) in the presence of 0.50 mmol of $TbCl_3 \times 6H_2O$ or $EuCl_3 \times 6H_2O$. The findings are even more surprising as the parity-forbidden *f→f* transitions of Tb^{3+} and Eu^{3+} are typically quenched in OH-containing solvents due to relaxation via O–H vibrations.

For excitation we have selected, on the one hand, the broad absorption of the C-dot at 275 nm for Tb^{3+}/PEG and 350 nm for Eu^{3+}/PEG (Fig. S9; *cf. main paper: Fig. 5*). In addition, excitation was performed via line-type *f→f* transitions of Tb^{3+} and Eu^{3+} at 366 and 390 nm, respectively (Fig. S9; *cf. main paper: Fig. 5*). Especially, excitation via the C-dot resulted in excellent quantum yields of 85 % for Tb^{3+}/PEG and 75 % for Eu^{3+}/PEG indicating a very efficient Förster resonance energy transfer (FRET) from the C-dot to the rare-earth metal. Notably, excitation of Tb^{3+}/PEG at 275 nm resulted in Tb^{3+}-related emission only, without any emission of the C-dot remaining.

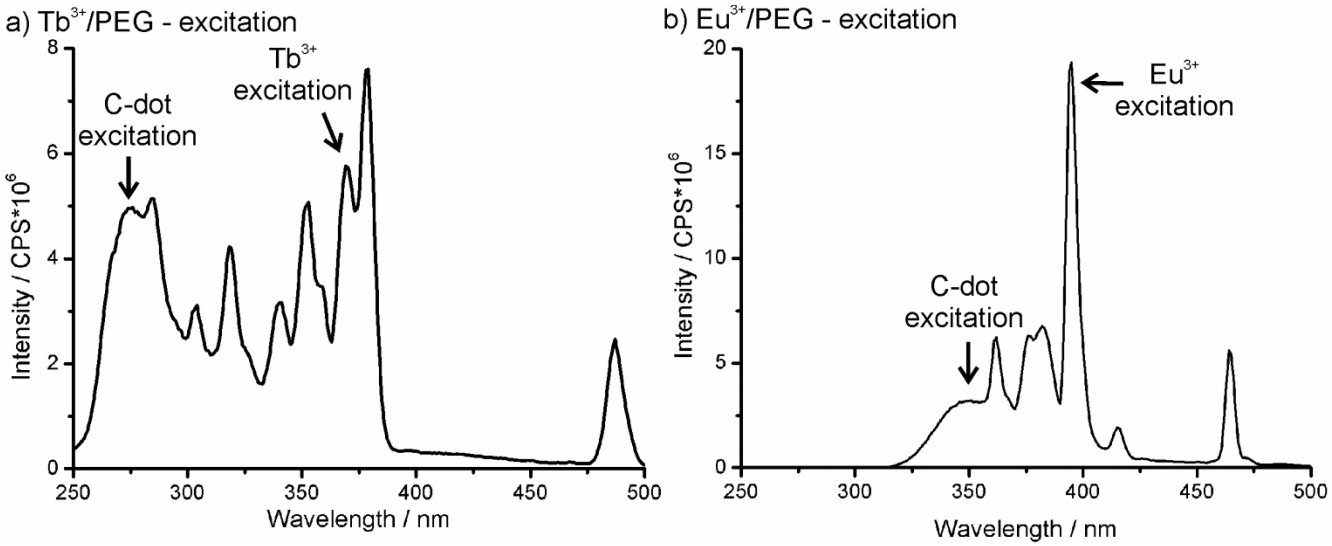

Figure S9. Excitation spectra of Tb^{3+}/Eu^{3+}-modified C-dots as obtained from refluxing PEG400: a) Tb^{3+}/PEG; b) Eu^{3+}/PEG. Excitation performed via the C-dot (275 and 350 nm) as well as via f→f transitions of the rare-earth metal (366 and 390 nm) (230 °C, 1 h, 0.5 mmol $TbCl_3 \times 6H_2O$/$EuCl_3 \times 6H_2O$; *cf. main paper: Fig5*).

Note that an efficient FRET essentially requires a close distance (<4 Å) between the corresponding luminescent centers (i.e. the C-dot and the rare earth ion).[4] The here presented C-dots are intrinsically surface functionalized by the polyol that served as the solvent. This polyol functionalization coordinates metal cations via its chelating oxygen functional groups. This finding has been described already in view of the formation and surface functionalization of C-dots.[5] If the cation coordinated by

the polyol-type surface functionalization is a rare-earth element, Förster resonance energy transfer is expected and obviously observed. The real surprise, however, is that energy-transfer and rare-earth emission are very efficient and even visible by the naked eye.

Since only Tb^{3+}/Eu^{3+} coordinated to the polyol-type surface functionalization can show efficient FRET and light emission, higher concentrations of Tb^{3+}/Eu^{3+} should not have any effect on the emission intensity if all available coordination sites at the C-dot surface are already occupied. As the relevant coordination sites can be considered as being located in a more-or-less mono-atomic coordination layer, the required concentration of Tb^{3+}/Eu^{3+} is comparably low. This was tested based on different concentrations of Tb^{3+}/Eu^{3+} in a range of 0.05 to 2.0 mmol (comparable to Mg^{2+}). As the C-dots are washed by repeated centrifugation and redispersion prior to suspension in D_2O and measuring the quantum yield, all Tb^{3+}/Eu^{3+} that was not coordinated by the polyol-type surface functionalization of the C-dots was removed. As a result, indeed no significant effect of different concentrations was observed in the studied range of 0.05 to 2.0 mmol. On the other hand, one has to consider secondary effects. As $TbCl_3/EuCl_3$ are Lewis-acids, their concentration can influence the nucleation and growth of the C-dots as well as their size and surface functionalization. This can also influence the emission of the C-dots without being an inherent effect of Tb^{3+}/Eu^{3+}. To this concern, much more detailed and systematic variations are necessary.

References

(1) a) J. V. de Mello, H. F. Wittmann and R. H. Friend, *Adv. Mater.* 1997, **9**, 230. b) S. Marks, J. Heck, P. O. Burgos, C. Feldmann and P. W. Roesky, *J. Am. Chem. Soc.* 2012, **134**, 16983.

(2) a) Y. Dong, H. Pang, H. B. Yang, C. Guo, J. Shao, Y. Chie, C. M. Li and T. Yu, *Angew. Chem. Int. Ed.* 2013, **52**, 7800. b) Y. Q. Zhang, D. K. Ma, Y. Zhuang, X. Zhang, W. Chen, L. L. Hong, Q. X. Yan, K. Yu and S. M. Huang, *J. Mater. Chem.* 2012, **22**, 16714. c) P. Trucano and R. Chen, *Nature* 1975, **258**, 136.

(3) a) S. Qu, X. Wang, Q. Lu, X. Liu and L. Wang, *Angew. Chem. Int. Ed.* 2012, **51**, 12215. b) A. Jaiswal, S. S. Gosh, A. Chattopadhyya, *Chem. Commun.* 2012, **48**, 407. c) W. Kwon and S. W. Rhee, *Chem. Commun.* 2012, **48**, 5256. d) X. Wang, K. Qu, B. Xu, J. Ren and X. Qu, *J. Mater. Chem.* 2011, **21**, 2445.

(4) a) J. Hohlbein, T. D. Craggs and T. Cordes, *Chem. Soc. Rev.* 2014, **43**, 1156 (Review). b) G. Blasse, C. Grabmaier, *Luminescent Materials*, Springer, Berlin 1994.

(5) a) S. Zhu, Q. Meng, L. Wang, J. Zhang, Y. Song, H. Jin, K. Zhang, H. Sun, H. Wang and B. Yang, *Angew. Chem. Int. Ed.* 2013, **52**, 3953. b) A. Jaiswal, S. S. Gosh and A. Chattopadhyya, *Chem. Commun.* 2012, **48**, 407.